Eng. & Tech. Journal, Vol.30 , No.13, 2012

Numerical and Experimental Prediction of Food Freezing

Dr. Jalal M. Jalil
Electromechanical Engineering Department, University of Technology/Baghdad
Email: jalamjalil@yahoo.com
Soundus S. AL-Azawi
Electromechanical Engineering Department, University of Technology/Baghdad

Received on: 28/9/2011 & Accepted on: 7/6/2012

ABSTRACT

In this study the freezing of foods was studied numerically and experimentally. Different kinds of foods have been studied numerically (Meat, Broccoli, Perch and Banana), while the experimental work is applied to meat only. In numerical solution enthalpy transformation method is used to transfer the energy equation into a non-linear equation with a single dependent variable E (enthalpy). The discretization of energy equation in three dimensions was solved with phase change problem employing the control-volume finite-difference. The numerical results of the enthalpy method were compared with experimental results and were satisfactory. The freezing process of foods differs from one to other due to thermal property differences, water content and freezing point. Low water content leads to smooth cooling rate and short constant temperature region while high water content leads to long constant temperature region.

Keywords: Food Freezing, Finite Volume, Enthalpy method, phase change

التنبوء العددي والعملي لانجماد الاغذية

الخلاصة

درس انجماد الاغذية في هذة الدراسة عدديا وعمليا. درست انواع عديدة من الاغذيـــة عـــدديا (اللحم، القرنابيط، السمك والموز). اما الدراسة العملية فقد تم تطبيقها على مادة اللحم. في الجانب النظري تم استخدام طريقة الانثالبي لتحويل معادلة الطاقة الى معادلة لاخطية مع متغير واحد هـــو الانثالبي. حلت معادلة الطاقة بالابعاد الثلاثية مع تغير الطور بواسطة الحجوم المحددة والفروقـــات المحددة. قورنت النتائج العددية للانثالبي مع النتائج العملية وكانت المقارنة مقبولة. كانـــت عمليـــة التجمد للاطعمة مختلفة من نوع الى الاخر اعتمادا على الخواص الحرارية، كمية المـــاء و نقطـــة الانجماد. كمية الماء القليلة قادت الى معدل تبريد ناعم و منطقة ثبوت درجة الحرارة صغيرة بينما كمية الماء الكبيرة تقود الى منطقة ثبوت درجة الحرارة طويلة.

https://doi.org/10.30684/etj.30.13.12
2412-0758/University of Technology-Iraq, Baghdad, Iraq

Nomenclature:

A	Area, m^2
a	coefficient in the discretization equation
b	coefficient in the discretization equation
c_p	specific heat, kJ/kg °C
c_{pl}	specific heat of liquid phase, kJ/kg °C
c_{ps}	specific heat of solid phase, kJ/kg °C
c_a	apparent specific heat, kJ/kg °C
c_i	food component specific heat, kJ/kg °C
E	Enthalpy, kJ/kg
E_f	enthalpy at initial freezing temperature, kJ/kg
H	latent heat, kJ/kg
k	thermal conductivity, W/ m °C
k_s	solid thermal conductivity, W/ m °C
k_l	liquid thermal conductivity, W/ m °C
k_i	component thermal conductivity, W/ m °C
T	Temperature, °C
T_m	melting temperature, °C
T^*	Kirchhoff temperature, °C
$\overline{T}$	reduced temperature= $\overline{T} = \frac{T - T_r}{T_f - T_r}$
V	Volume, m^3
x_b	mass fraction of bound water
x_i	mass fraction of food component
x,y,z	Cartesian coordinates, m
x_i^v	Volume fraction of constituent i
y	correlation parameter
t	Time, s
ρ	Density, kg/m^3
E,W,N,S,T,B	Neighbors
e,w,n,s,t,b	control volume face neighbors

INTRODUCTION

Transient heat transfer problems involving melting or solidification is generally referred to as phase change or moving boundary problems. Fluid flow and thermal effects during melting and solidification are of great importance in many industrial applications. Its main characteristic is that the moving interface separates two phases with different physical properties. The solution of such problems is inherently difficult because the interface between the solid and liquid

phases moves as the latent heat is absorbed or released at the interface; as a result, the location of the solid-liquid interface is unknown a prior.

There are different methods for studying heat transfer with phase change materials; enthalpy method was the most appropriate. It was used by many researchers. For example, (Bomben, 1982) studied the heat and mass transport in freezing of apple tissue, (Pham, 1986) has formulated a simplified equation for predicting the freezing time for food staff and (Chau, 1988) developed equations to describe the transpiration of fruit. (Sheen, 1991) build a mathematical model including the volumetric changes for food freezing or thawing is obtained by modifying the general heat conduction parabolic partial differential equation. (Hossain, 1992) shows a new expression for a geometric factor for ellipsoid shapes is developed by applying semi-analytical solutions of phase-change problems with convective cooling at the surface. More recently, (Shatikian, 2003) explored numerically the melting and solidification of PCM (paraffin wax), (Scanlon, 2004) studied the food freezing and melting with natural convection, (Stritih, 2004) studied the heat transfer enhancement due to natural convection in thermal storage, (Kalaiselvam 2008) studied experimentally and analytically melting and solidification of PCM inside cylindrical encapsulation and finally (Nortan 2009) used enthalpy method for simulating of high pressure freezing.

In this study, an enthalpy-transforming scheme is proposed to convert the energy equation into a non-linear equation with enthalpy, E, being the single dependent variable. The existing control-volume finite-difference approach is simplified so it can be applied to the three-dimensional numerical performance of Stefan problems. The present research deals with the freezing process of different kinds of foods numerically like (Meat, Broccoli, Perch and Banana). Experimentally only freezing of the meat was studied. The main aim of the experimental and numerical works is to find out the temperature distributions inside food with the change of phase and the position of interface between liquid and solid with time, which leads to find out the time required for freezing the food.

STEFAN PROBLEM WITH ENTHALPY TRANSFORMING METHOD

Stefan problems represented heat conduction problems with phase change. This problem is treated by the enthalpy transforming method, where this method is proposed to convert the energy equation into a non-linear equation with the enthalpy (E), being the single dependent variable. The advantage of the enthalpy reformulation is that the problem to be solved is formulated in a fixed region. The enthalpy method treats the enthalpy as a dependent variable in addition to temperature, and discretizes the energy equation into set of equations that contains both enthalpy and temperature. The assumptions of the analysis are:

1. no viscous dissipation
2. neglecting convection term
3. constant specific heats for each phase where the phase change occurs at a single temperature

The three-dimensional analysis of the model is related to Cao, 1989. The energy equation is as follows

$$\frac{\partial}{\partial x}\left(k\frac{\partial T}{\partial x}\right)+\frac{\partial}{\partial y}\left(k\frac{\partial T}{\partial y}\right)+\frac{\partial}{\partial z}\left(k\frac{\partial T}{\partial z}\right)=r\frac{\partial E}{\partial t} \qquad (1)$$

With the state equation,

$$\frac{dE}{dT} = C_p(T) \qquad (2)$$

The temperature is calculated from the equation below for solid, interface and liquid region.

$$T \begin{cases} T_m + E/Cp_s & E \le 0 \quad \text{(Solid region)} \\ T_m & 0 < E < H \quad \text{(Interface region)} \\ T_m + (E-H)/Cp_l & E \ge H \quad \text{(Liquid region)} \end{cases} \qquad (3)$$

T_m is the melting or freezing temperature. In the above relation, E = 0 corresponding to phase change materials in their solid state to temperature T_m. The (Kirchhoff temperature) definition is introduced as follows:

$$T^* = \begin{cases} k_s(T-T_m) & T < T_m \quad \text{(Solid region)} \\ 0 & T = T_m \quad \text{(Interface region)} \\ k_l(T-T_m) & T > T_m \quad \text{(Liquid region)} \end{cases} \qquad (4)$$

Transforming equations (3) with the definition given in equation (4) yields,

$$T^* = \begin{cases} k_s E/Cp_s & E \le 0 \quad \text{(Solid region)} \\ 0 & 0 < E < H \quad \text{(Interface region)} \\ k_l(E-H)/Cp_l & E \ge H \quad \text{(Liquid region)} \end{cases} \qquad (5)$$

Now enthalpy function can be introduce as follows,

$$T^* = \Gamma(E)E + S(E) \qquad (6)$$

For the phase change occurring at a single temperature, the coefficients (Γ, S) are given in the following equations.

$$\Gamma(E) = \begin{cases} k_s / Cp_s & E \le 0 \quad \text{(Solid region)} \\ 0 & 0 < E < H \quad \text{(Interface region)} \\ k_l / Cp_l & E \ge H \quad \text{(Liquid region)} \end{cases} \qquad (7)$$

$$S(E)=\begin{cases} 0 & E \le 0 \quad \text{(Solid region)} \\ 0 & 0 < E < H \quad \text{(Interface region)} \\ -Hk_l / Cp_l & E \ge H \quad \text{(Liquid region)} \end{cases} \tag{8}$$

Transforming equation 1 in-terms of Kirchoff temperature, and substituting using equation 6, gives:

$$r\frac{\partial E}{\partial t}=\frac{\partial}{\partial x}\left(\frac{\partial(\Gamma E)}{\partial x}\right)+\frac{\partial}{\partial y}\left(\frac{\partial(\Gamma E)}{\partial y}\right)+\frac{\partial}{\partial z}\left(\frac{\partial(\Gamma E)}{\partial z}\right)+p \tag{9}$$

With

$$p=\frac{\partial}{\partial x}\left(\frac{\partial S}{\partial x}\right)+\frac{\partial}{\partial y}\left(\frac{\partial S}{\partial y}\right)+\frac{\partial}{\partial z}\left(\frac{\partial S}{\partial z}\right) \tag{10}$$

In the liquid region away from the moving front equation (1) it is reduced to the normal linear energy equation

$$r\frac{\partial E}{\partial t}=\frac{\partial}{\partial x}\left(k_l\frac{\partial T}{\partial x}\right)+\frac{\partial}{\partial y}\left(k_l\frac{\partial T}{\partial y}\right)+\frac{\partial}{\partial z}\left(k_l\frac{\partial T}{\partial z}\right) \tag{11}$$

Also in the solid region equation (1) it is reduced to

$$r\frac{\partial E}{\partial t}=\frac{\partial}{\partial x}\left(k_s\frac{\partial T}{\partial x}\right)+\frac{\partial}{\partial y}\left(k_s\frac{\partial T}{\partial y}\right)+\frac{\partial}{\partial z}\left(k_s\frac{\partial T}{\partial z}\right) \tag{12}$$

The discretization of equations (9, 11, and 12) is obtained by applying conservation laws over finite size control volume surrounding the grid nodes, and by integrating the equation over the control volumes i.e.

$$\iiint_{\Delta V} r\frac{\partial E}{\partial t}\Delta V=\iiint_{\Delta V}\frac{\partial}{\partial x}\left(\frac{\partial(\Gamma E)}{\partial x}\right)\Delta V+\iiint_{\Delta V}\frac{\partial}{\partial y}\left(\frac{\partial(\Gamma E)}{\partial y}\right)\Delta V+\iiint_{\Delta V}\frac{\partial}{\partial z}\left(\frac{\partial(\Gamma E)}{\partial z}\right)\Delta V$$

$$+\iiint_{\Delta V}\frac{\partial}{\partial x}\left(\frac{\partial S}{\partial x}\right)\Delta V+\iiint_{\Delta V}\frac{\partial}{\partial y}\left(\frac{\partial S}{\partial y}\right)\Delta V+\iiint_{\Delta V}\frac{\partial}{\partial z}\left(\frac{\partial S}{\partial z}\right)\Delta V \tag{13}$$

Using an explicit scheme, the time variation term becomes,

$$\iiint_{\Delta V} r \frac{\partial E}{\partial t} \Delta V = r \Delta V \left(\frac{E_p - E_p^{\circ}}{\Delta t} \right) \quad (14)$$

The first term for x-direction of Equation (9) becomes

$$\iiint_{\Delta V} \frac{\partial}{\partial x} \left(\frac{\partial (\Gamma E)}{\partial x} \right) \Delta V = \left[\left(\frac{\partial (\Gamma E)}{\partial x} \right)_e - \left(\frac{\partial (\Gamma E)}{\partial x} \right)_w \right] \Delta y \ \Delta z \quad (15)$$

Now transforming Equation (9) to the familiar standard form gives:

$$E_P = a_N E_N + a_S E_S + a_E E_E + a_W E_W + a_T E_T + a_B E_B + b \quad (16)$$

Where'

$$b = -[a_P - 1] E_P^{\circ} + b_N S_N + b_S S_S + b_E S_E + b_W S_W + b_T S_T + b_B S_B - b_P S_P \quad (17)$$

$$a_p = a_E + a_W + a_N + a_S + a_T + a_B \quad (18)$$

$$b_p = b_E + b_W + b_N + b_S + b_T + b_B \quad (19)$$

$$a_N = \frac{\Delta t \ \Gamma_N \ A_y}{r \ \Delta V \ dy_N} \quad (20)$$

$$A_x = \Delta y \ \Delta z, \qquad A_y = \Delta x \ \Delta z, \qquad A_z = \Delta x \ \Delta y, \qquad \Delta V = \Delta x \ \Delta y \ \Delta z \quad (21)$$

Similarly for equations 11 and 12 for liquid and solid regions

Thermal Properties of Foods

Thermo-physical properties of foods and beverages that are often required for heat transfer calculation include density, specific heat, enthalpy and thermal conductivity

Density: Modeling the density of foods and beverages requires knowledge of the food porosity, as well as the mass fraction and density of the food components. The density r of foods and beverages can be calculated accordingly:

$$r = \frac{(1 - e)}{\sum x_i / r_i} \quad (22)$$

The porosity (ε) is required to model the density of granular food items stored in bulk, such as grains and rice. For other food items, the porosity is zero.

Specific Heat: it is a measure of the energy required to change the temperature of a food item by one degree and can be calculated as follows:

$$c_p = \sum c_i \ x_i \quad (23)$$

Thermal Conductivity: it relates the conduction heat transfer rate to the temperature gradient

$$k = \frac{1}{\sum (x_i^v / k_i)} \tag{24}$$

Tables 1, 2, 3 and 4 show the details thermal properties used in this study; the properties are updated with temperature at each time step.

Boundary Conditions

In order to begin the computations, initial conditions have to be set at time t = 0. These initial conditions are specified at all grid points for dimensional variables. The initial conditions for internal grid points are fresh food (liquid state) with 20 ºC while different values of surface temperatures are tested (-10, -15 and -20) as shown in Table 5. Only one-eighth of the cube was studied due to symmetry. The boundary conditions are:

At x = 0 surface, gradient zero due to symmetry, $\frac{\partial T}{\partial x} = 0$

At y = 0 surface, gradient zero due to symmetry, $\frac{\partial T}{\partial y} = 0$

At z = 0 surface, gradient zero due to symmetry, $\frac{\partial T}{\partial z} = 0$

At x = l surface, T = T_c (isothermal cold surface), Table 5
At y = l surface, T = T_c (isothermal cold surface), Table 5
At z = l surface, T = T_c (isothermal cold surface), Table 5
L = length of the cube.

Special boundary conditions were used to simulate the experimental test condition, the experimental surface temperature readings were taken from experimental result to use in the program as input to calculate the internal temperature distribution inside the cube.

EXPERIMENTAL WORK

The test unit is designed and fabricated to examine the numerical results that obtained by solving the problem of freezing of meat in three dimensional Cartesian coordinates, the main parts of this unit are:

1. A cubic shape basket made from steel wire coated by plastic and has a dimension 20*20*20 cm, Figure 1.
2. Thermocouples, Copper-constant thermocouples were used for temperature measurement. The thermocouple wires were of 0.46 mm diameter fixed inside meat and distributed in uppesr left quarter from the block, Figure 2 shows the calibration curve for thermocouples, the type which used for this purpose is T. Twenty seven thermocouples were fixed inside meat basket at a distance of 2.5 cm between them, in three-dimension. Also three thermocouples fixed in three surface of the cube.

3. Selector Switch, two selector switch of multi points for each one have 20 points were used for connecting the thermocouples to the digital thermometer.
4. Digital thermometer, One Comark electronic thermometer, range -60 to 170 °C. Accuracy at 23 °C is 0.5 °C.
5. Digital Anemometer which is used to measure air velocity.
   The experimental work was done inside cold storage room has the dimension 4*3.5*1.8 m. It is inside big super market. This room is used for different types of food storage, e.g. meat, fish and chicken. The refrigeration machine which is used in experimental work is designed to provide safe convectional cold storage room. The cold storage room capacity is 5 tons of refrigeration, the circulated air in the room has velocity of 4.5 m/s, the temperature of the air at the exit from the refrigeration machine is -10 °C.

EXPERIMENTAL PROCEDURE

A cubic shape of basket (20*20*20) cm is used filled with meat; both basket and meat are placed in a cold storage room to freeze the meat. Copper-constant thermocouple wires type T are inserted in the upper left eighth (symmetries) of the cubic shape to read temperature distribution. The chosen points and distribution for the temperature measuring are shown in Figure 1. The measurements will be repeated at different time intervals until reaching the state where meat is fully frozen. The cold storage room (4*3.5*1.8 m) is supplied with air at low temperature; which circulates around meat block and causes the freezing. The main aim of the experimental work is to find out the temperature distributions inside meat with change of phase and the position of interface between liquid and solid with time, which lead to find out the time required for freezing the meat. The thermocouple reading was calibrated with thermometer readings. The initial temperature of meat block was recorded, and then the meat block with its thermocouples was placed in the cold storage room, at this time the freezing process was started. All points' temperature is recorded with time until all points readings are less than 0.1 ºC. This indicates the block of meat was frozen.

RESULTS AND DISCUSSION

The main objective of this paper is to find out the required time for freezing meat, some kinds of fruit and vegetable and also to locate the interface between liquid and solid at each time. Numerical and experimental simulations of the frozen meat block in dimensions (20*20*20 cm) are studied. In the experimental work the block of meat at an initial temperature of 20 °C and the cold storage room at –9 °C, numerically same experimental initial and boundary conditions are used. Figure 3 represents the isothermal contours for experimental and numerical works at different time intervals. Only eighth volume of the cube was shown in the figure, and the point (x=0, y=0, z=0) represents center of the cube, which have the highest temperature (nearly orange colure). All the temperature decreases with the time and the boundary surface temperatures have the lowest temperatures (blue color). The agreement between experimental and numerical results seems acceptable. The reason for the differences

is the natural convection in the experimental work, which is negligible in numerical work.

Figure 4 displays a comparison between the experimental and numerical work for selected points. The numerical results shows clear latent heat removing at 0 C in

points 2 and 3 while a change of cooling curve slope for points 4, 5 and 1at 0 C. The deviation of points 4, 5 and 1 from points 2 and 3 behavior is due to boundary effect. For experimental results, the only explanation is that the natural convection mixes the two behaviors and the results only show a change of cooling curve slope at 0 C for all points. It is noticed that at time = 0, the points have the same values for both numerical and experimental work. For time > 0, the numerical values are above the experimental curve because the natural convection effect in numerical work was neglected but in the experimental work it exists. The difference between numerical and experimental decreases as the points approach the boundary area (points 1 and 5) and increases when the point is away from boundary area (points 2, 3 and 4). This is because the boundary temperatures for numerical solution come from experimental data. At point 1, the numerical results are higher than the experimental results along the time with 9.11%, and for point 3 it's 13.4 %, while at points 5 the difference approaches 8.25%.

Figure 5 shows the numerical temperature contour for broccoli cube block, length of the cubic which is 0.1 m, melting temperature, t_m = – 0.6 °C and the surface temperature is -15°C. The figure shows the decrease of temperatures with time. The lowest temperature is located in the lower right corner, where it reaches nearly 0 °C at 4 hours, -10 °C at 8 hours and -15 °C at 9.5 hours. Figure 6 shows the variation of temperature with time for selected points in the center of broccoli block. Different surface temperatures are tested -10 °C, -15 °C and -20 °C. The block length was 0.15 m. The interface position in this figure is stable and occurs at temperature -0.6 °C at time equal to 7.5 hours for surface temperature -10°C, 5 hours for surface temperature -15 °C and 3.5 hours for surface temperature -20 °C. This indicates that freezing time increases with the decrease of surface boundary temperature.

Figure 7 shows temperature variation with time for selected points in the center of broccoli block. Different lengths of the cubic are tested, 0.1, 0.15 and 0.2 m. The surface temperature is -15 °C. The interface position in this figure is stable and occurs nearly at -0.6° C with time equal to 2 hours for 0.1 m, 10 hours for 0.15 and 17 hours for 0.2 m. This indicates the freezing time increases with the increase of block size.

Figure 8 shows the temperature variation with time for different kinds of foods, meat, banana, broccoli and perch at the center of the block. The length of block is 0.2 m and surface temperature is -20 °C. The position of interface is differs from one to another because of the different quantity of water content and latent heat; for Broccoli water content is equal to 90% and the latent heat is equal to 301 kJ/kg, Banana; water content is equal to 75% and latent heat is equal to 251 kJ/kg, meat; water content is equal to 45% and the latent heat is equal to 251 kJ/kg. Finally for perch; the water content is equal to 80% and the latent heat is equal to 267 kJ/kg [Ashrae 1998]. The constant temperature region will depend on water content. Broccoli shows longest constant temperature because of high water content while meat shows shortest constant temperature region because of low water content. The water content delays the freezing process so Broccoli have slowest cooling rate while the meat have fastest rate.

CONCLUSIONS

The most important conclusions of the present research are:

1. The present work predicts locations of interface and temperature with time for different foods, surface temperatures and block sizes.
2. The freezing of foods differs from one type to another because of water content and different thermal properties. Meat seems the fastest then Banana, Perch and last is the Broccoli.
3. Constant temperature region will depend on water content, Meat will have nearly smooth cooling rate due to low water content while Broccoli will have clear constant temperature region due to high water content.
4. A comparison between experimental and numerical results gives good agreement, showing that the present model can properly predict the phase change processes.

REFERENCES

[1]Ashrae Refrigeration Hand Book, 1998.

[2]Bomben J. L. and King C. J., (1982). Heat and Mass Transport in the Freezing of Apple Tissue, J. Food Technology, Vol. 17, PP. 615-632.

[3]Cao Y. and Faghri A., (1989), A numerical analysis of Stefan problems for generalized multi-dimensional phase change structure using the enthalpy transformation model, J. Heat Mass Transfer, Vol. 32, No. 7, PP. 1289-1298.

[4]Chau K. V., Gaffney J. J., and Romero R. A., (1988). A Mathematical Model for the Transpiration from Fruits and Vegetables, Ashrae Transactions, Vol. 94, PP: 1541-1552.

[5]Hossain Md. M., Cleland D. J. and Cleland A. C., (1992). Prediction of freezing and thawing times for foods of three-dimensional irregular shape by using a semi-analytical geometric factor, Int. J. Refrigeration, Vol. 15, PP: 241-246.

[6]Kalaiselvam S., Veerappan M., Arul Aaron A. and Iniyan, S., (2008), Experimental and analytical investigation of solidification and melting characteristics of PCMs inside cylindrical encapsulation, Int. J. Thermal Sciences Vol. 47, PP: 858-874.

[7]Norton T., Delgado A., Hogan E., Grace P. and Sun D., (2009), Simulation of high pressure freezing processes by enthalpy method, J. Food Engineering, Vol. 91, PP: 260-268.

[8]Pham Q. T., (1986). Simplified Equation for Predicting the Freezing Time of Food Stuffs, J. Food Technology, Vol. 21, PP: 615-622.

[9]Scanlon T.J. and Stickland M.T., (2004), A numerical analysis of buoyancy-driven melting and freezing, Int. J. Heat Mass Transfer, Vol. 47, PP: 429-436.

[10]Shatikian V., Dubovsky G., Ziskind G. and Letan R., (2003), Simulation of PCM Melting and Solidification in a Partitioned Storage Unit, ASME Summer Heat Transfer Conference.

[11]Sheen S. and Hayakawa K.I., (1991). Finite difference simulation for heat conduction with phase change in an irregular food domain with volumetric change, International Journal of Heat and Mass Transfer, Vol. 34, PP: 1337-1346.

[12]Stritih U., (2004). An experimental study of enhanced heat transfer in rectangular PCM thermal storage, Int. J. Heat Mass Transfer, Vol. 47, PP: 2841-2847.

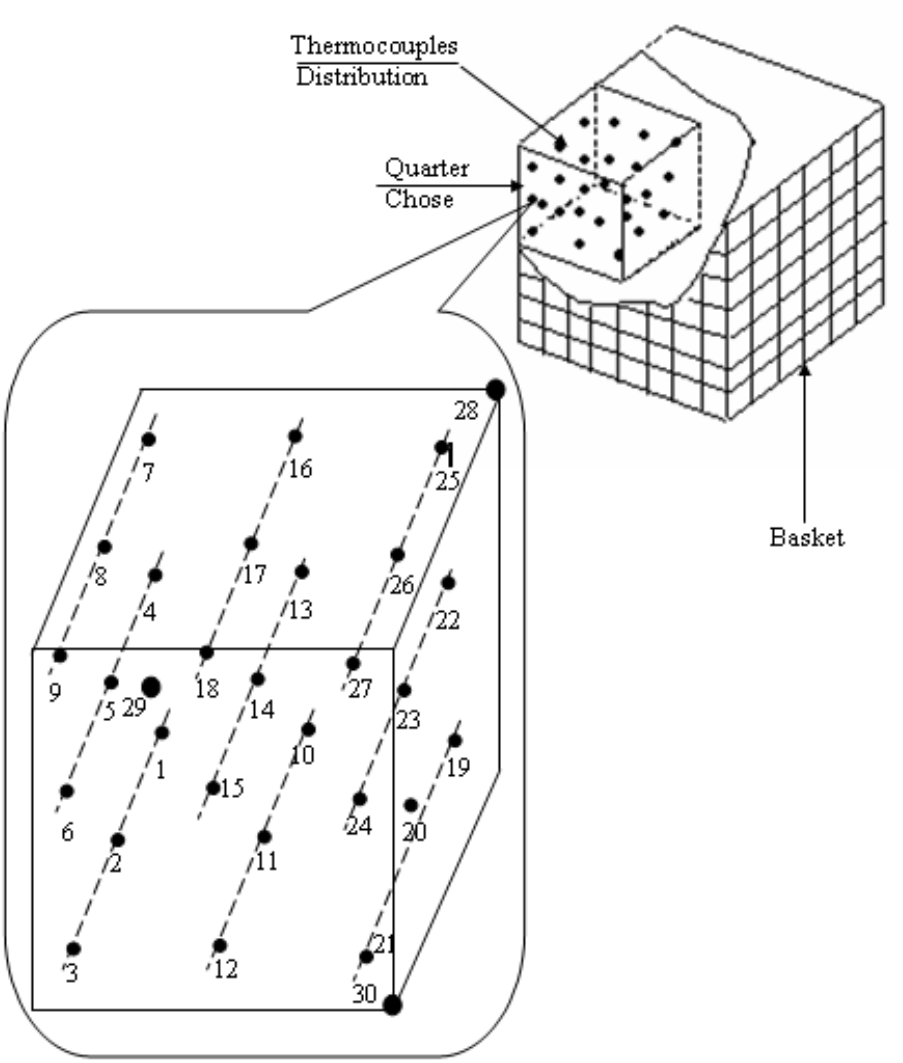

Figure (1) Chosen points and distribution for temperature measuring.

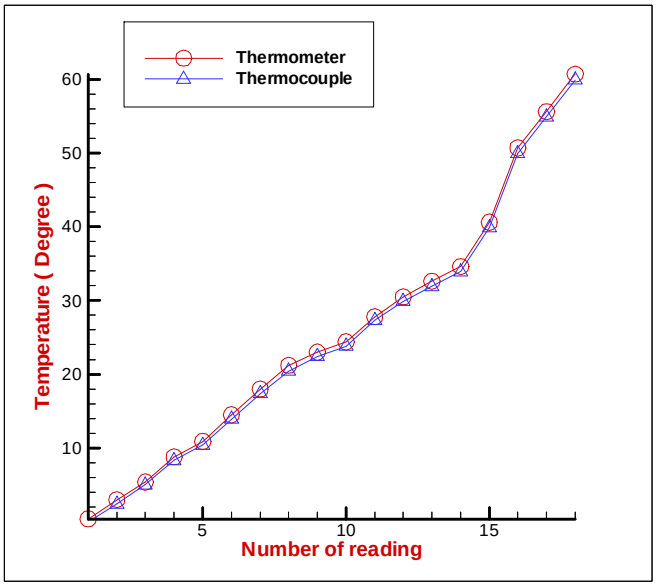

Figure (2) The Calibration Curve

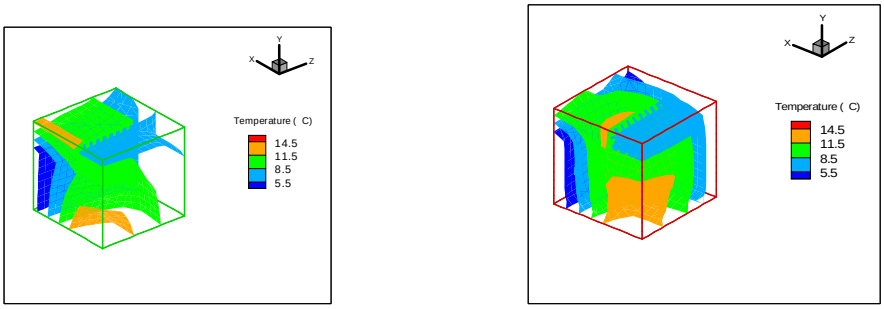

Time =1 hours

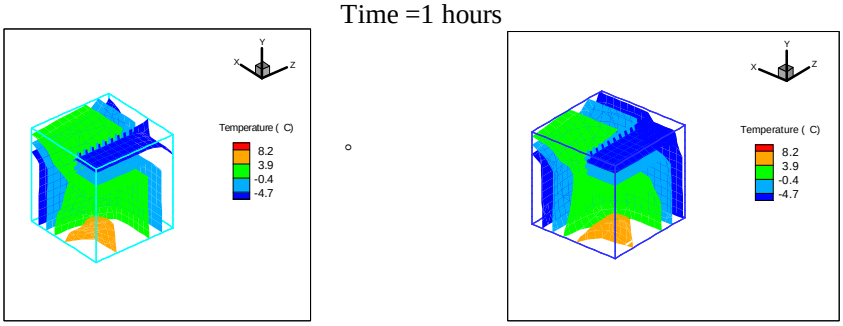

Time = 3 hours

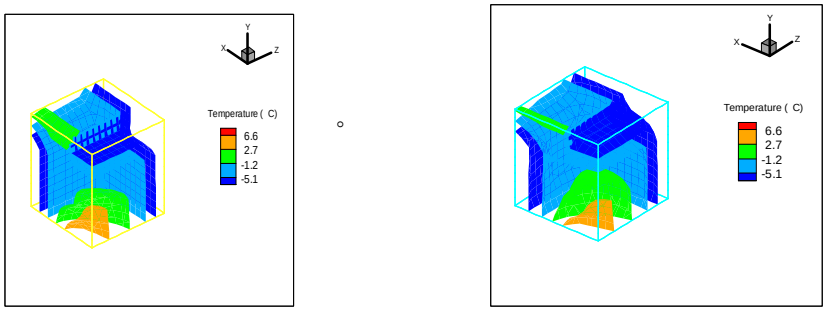

Time = 4 hours

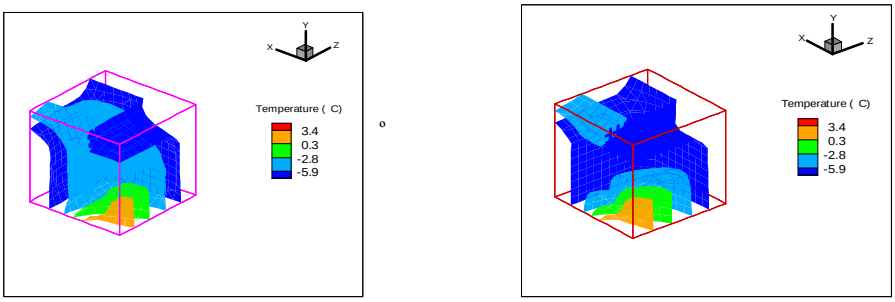

Time = 6 hours

Experimental Numerical

Figure 3 Transient comparisons between numerical and experimental results.

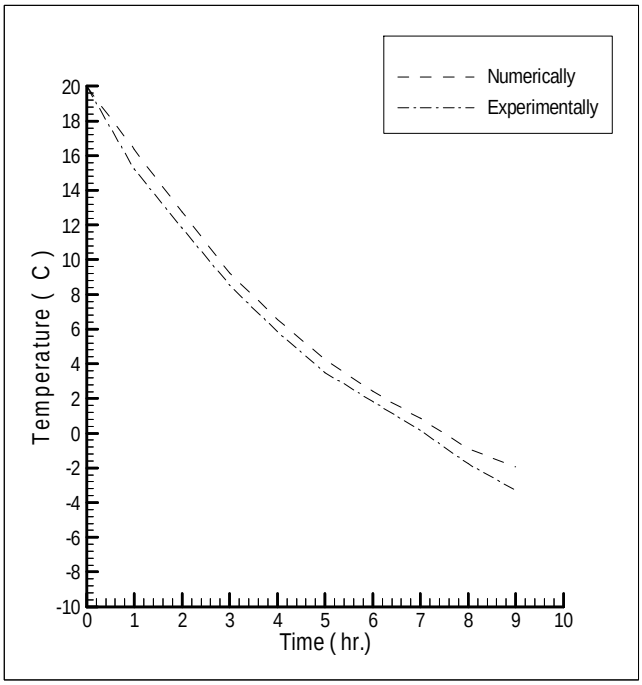

A) POINT 1, Position x = 0.1/6 m, y = 0.1/6 m, z = 0.1/6 m

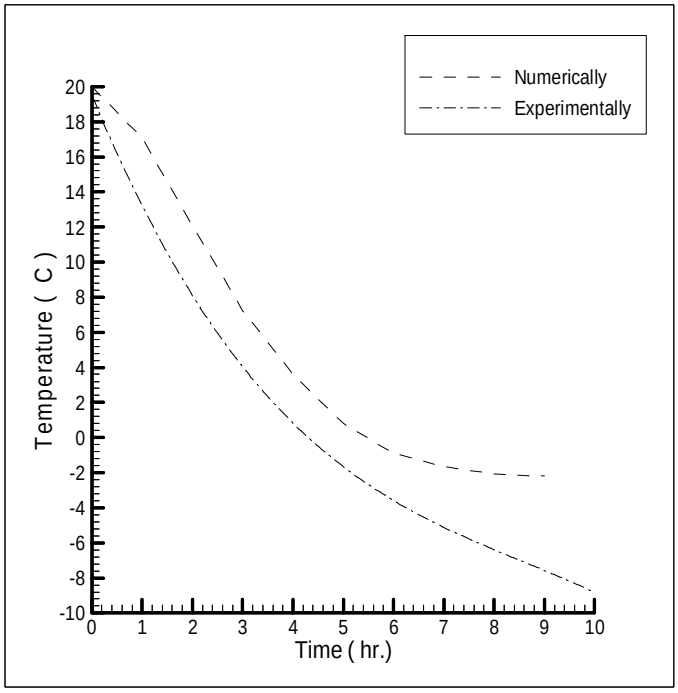

B) POINT 2, Position x = (2*0.1)/6 m, y = (2*0.1)/6 m, z = (2*0.1)/6 m

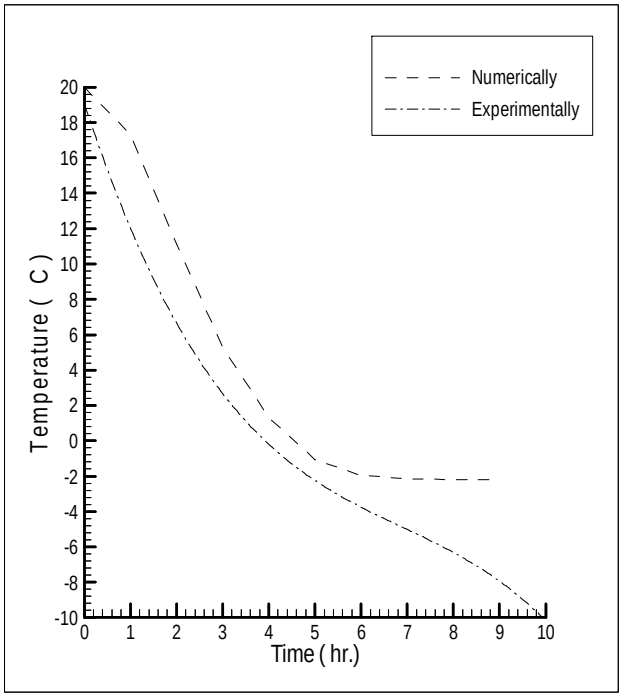

C) POINT 3, Position, x = (3*0.1)/6 m, y = (3*0.1)/6 m, z = (3*0.1)/6 m

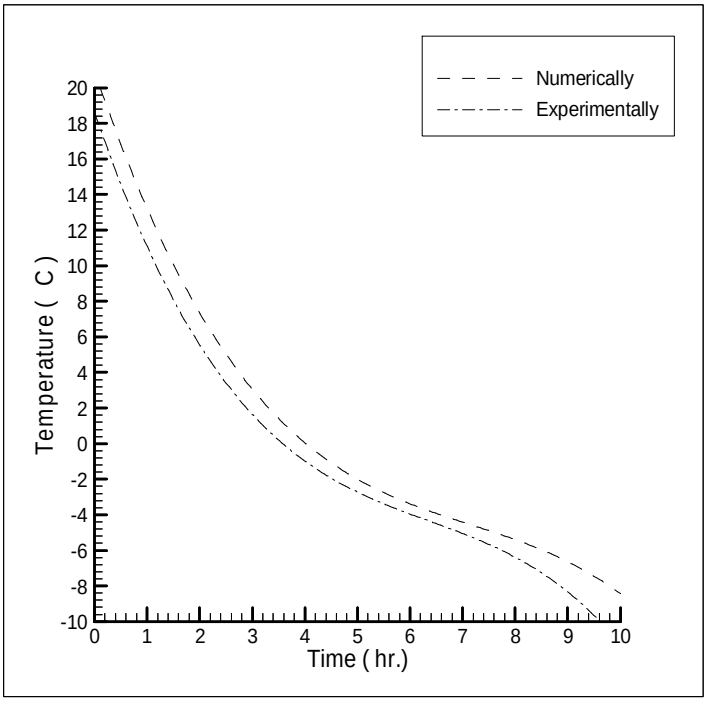

D) POINT 4, Position x = (4*0.1)/6 m, y = (4*0.1)/6 m, z = (4*0.1)/6 m

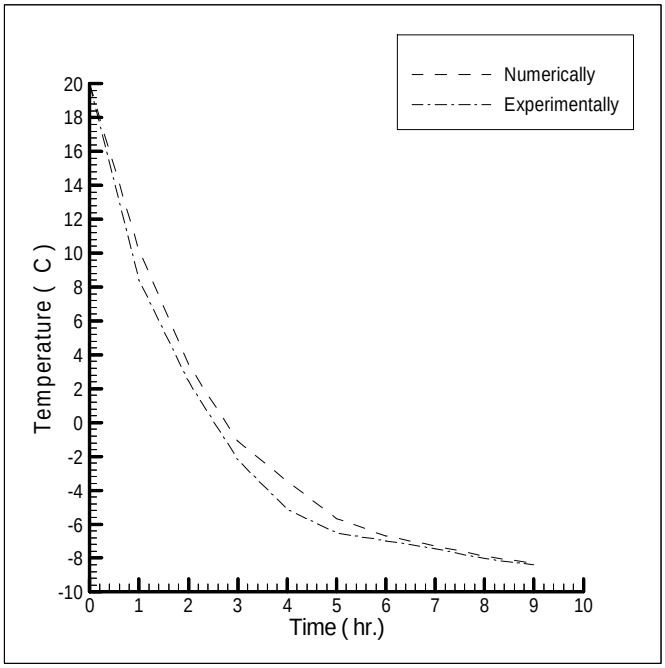

E) **POINT 5, Position x = (5*0.1)/6 m, y = (5*0.1)/6 m, z = (5*0.1)/6 m**

Figure (4) Numerical and experimental temperature variation with time for selected points

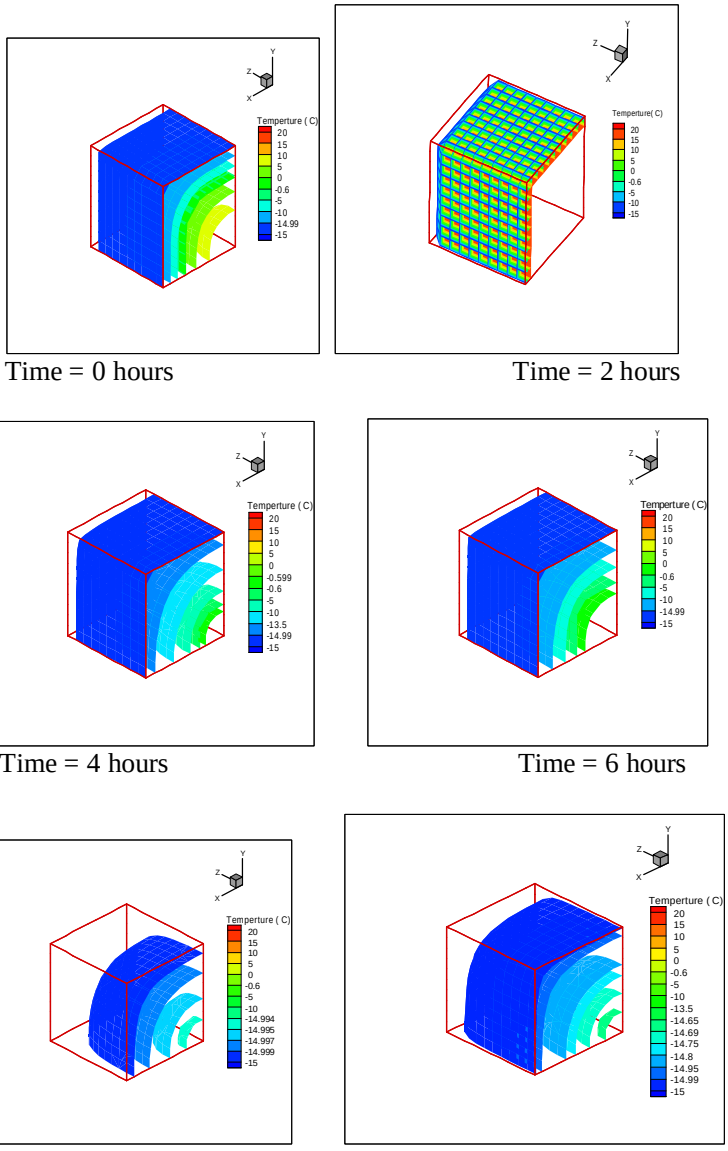

Figure (5) Transient numerical isothermal contours for Broccoli block

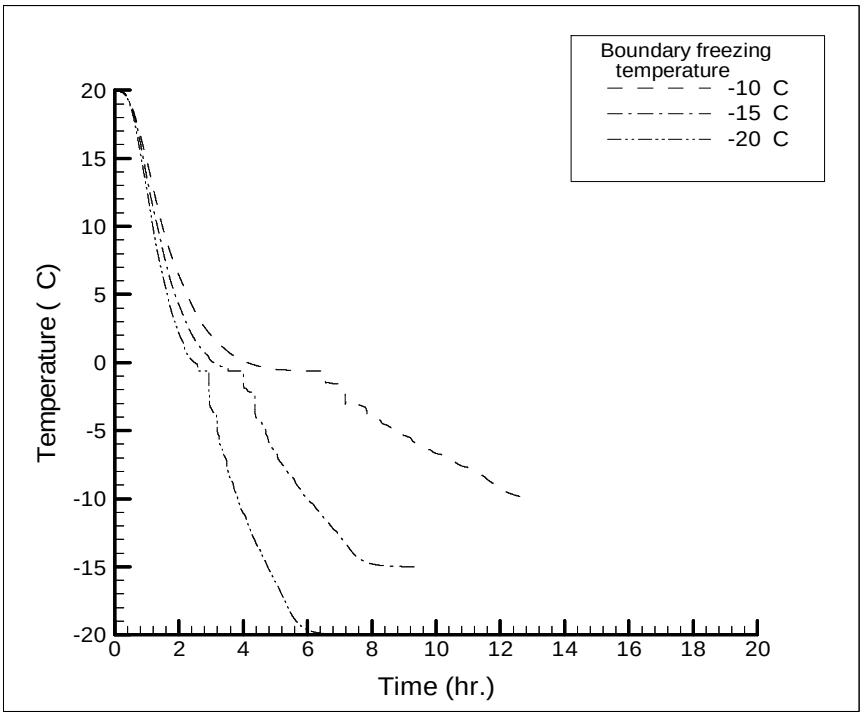

Figure(6) Central point temperature variation with time for different Boundaries for broccoli for (L = 0.15 m)

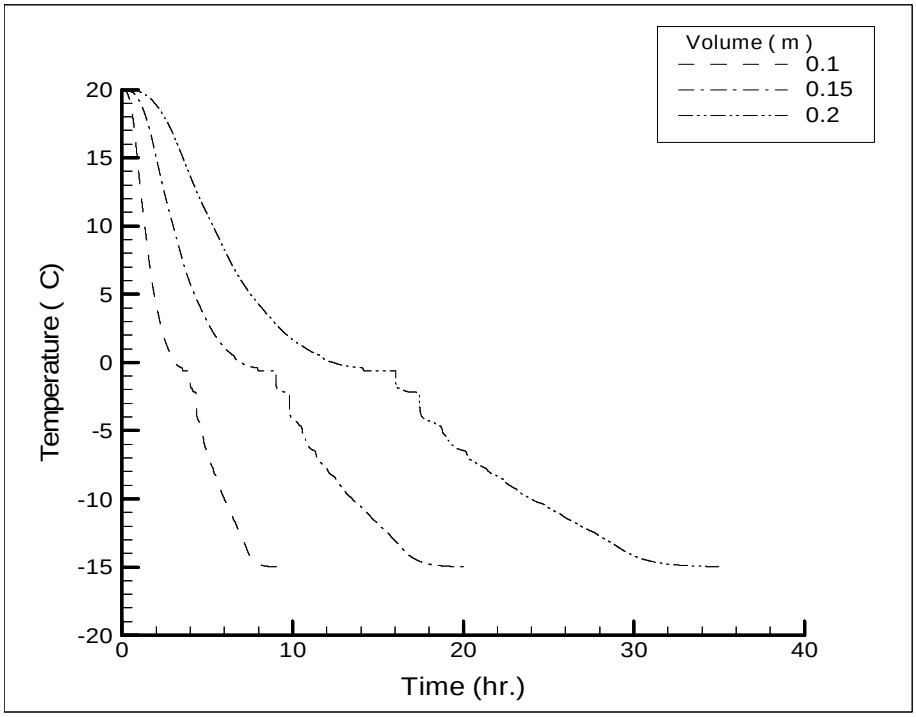

Figure (7) central point temperature variations with time For different block sizes for broccoli at (T = -15 ºC).

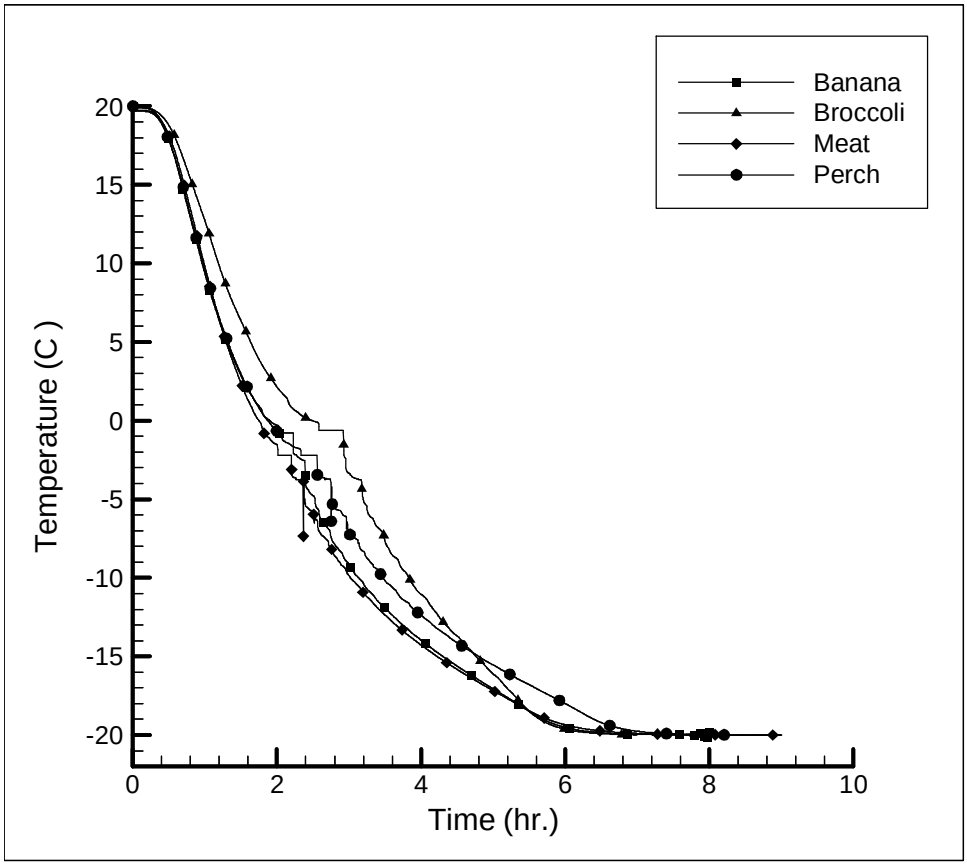

Figure (8) Central point temperature variations with time For different kinds of food, Length of block is 0.2 m and surface temperature is -20 ºC.

Table (1) Thermal Properties Models for Food Components (-40°C ≤ *T* ≤ 150°C) [Ashrae 1998]

Items	Thermal Property	Food Component	Thermal Property Model
1	Thermal conductivity, W/(m·K)	Protein	$k = 1.7881 \times 10^{-1} + 1.1958 \times 10^{-3}T - 2.7178 \times 10^{-6}T^2$
		Fat	$k = 1.8071 \times 10^{-1} - 2.7604 \times 10^{-3}T - 1.7749 \times 10^{-7}T^2$
		Carbohydrate	$k = 2.0141 \times 10^{-1} + 1.3874 \times 10^{-3}T - 4.3312 \times 10^{-6}T^2$
		Fiber	$k = 1.8331 \times 10^{-1} + 1.2497 \times 10^{-3}T - 3.1683 \times 10^{-6}T^2$
		Ash	$k = 3.2962 \times 10^{-1} + 1.4011 \times 10^{-3}T - 2.9069 \times 10^{-6}T^2$
2	Thermal diffusivity, m2/s	Protein	$\alpha = 6.8714 \times 10^{-2} + 4.7578 \times 10^{-4}T - 1.4646 \times 10^{-6}T^2$
		Fat	$\alpha = 9.8777 \times 10^{-2} - 1.2569 \times 10^{-4}T - 3.8286 \times 10^{-8}T^2$
		Carbohydrate	$\alpha = 8.0842 \times 10^{-2} + 5.3052 \times 10^{-4}T - 2.3218 \times 10^{-6}T^2$
		Fiber	$\alpha = 7.3976 \times 10^{-2} + 5.1902 \times 10^{-4}T - 2.2202 \times 10^{-6}T^2$
		Ash	$\alpha = 1.2461 \times 10^{-1} + 3.7321 \times 10^{-4}T - 1.2244 \times 10^{-6}T^2$
3	Density, kg/m3	Protein	$\rho = 1.3299 \times 10^{3} - 5.1840 \times 10^{-1}T$
		Fat	$\rho = 9.2559 \times 10^{2} - 4.1757 \times 10^{-1}T$
		Carbohydrate	$\rho = 1.5991 \times 10^{3} - 3.1046 \times 10^{-1}T$
		Fiber	$\rho = 1.3115 \times 10^{3} - 3.6589 \times 10^{-1}T$
		Ash	$\rho = 2.4238 \times 10^{3} - 2.8063 \times 10^{-1}T$
4	Specific heat, kJ/(kg·K)	Protein	
		Fat	$c_p = 2.0082 + 1.2089 \times 10^{-3}T - 1.3129 \times 10^{-6}T^2$
		Carbohydrate	$c_p = 1.9842 + 1.4733 \times 10^{-3}T - 4.8008 \times 10^{-6}T^2$
		Fiber	$c_p = 1.5488 + 1.9625 \times 10^{-3}T - 5.9399 \times 10^{-6}T^2$
		Ash	$c_p = 1.8459 + 1.8306 \times 10^{-3}T - 4.6509 \times 10^{-6}T^2$
			$c_p = 1.0926 + 1.8896 \times 10^{-3}T - 3.6817 \times 10^{-6}T^2$

Table (2) Thermal Property Models for Water and Ice (-40°C £ *T* £ 150°C) [Ashrae 1998]

Items	Thermal Property	Thermal Property Model
Water	Thermal conductivity, W/(m·K) Thermal diffusivity, m2/s Density, kg/m3 Specific heat, kJ/(kg·K) (For temp. range of –40°C to 0°C) Specific heat, kJ/(kg·K) (For temp. range of 0°C to 150°C)	$kw = 5.7109 \times 10^{-1} + 1.7625 \times 10^{-3}T - 6.7036 \times 10^{-6}T^2$ $\alpha w = 1.3168 \times 10^{-1} + 6.2477 \times 10^{-4}T - 2.4022 \times 10^{-6}T^2$ $\rho w = 9.9718 \times 10^2 + 3.1439 \times 10^{-3}T - 3.7574 \times 10^{-3}T^2$ $cw = 4.0817 - 5.3062 \times 10^{-3}T + 9.9516 \times 10^{-4}T^2$ $cw = 4.1762 - 9.0864 \times 10^{-5}T + 5.4731 \times 10^{-6}T^2$
Ice	Thermal conductivity, W/(m·K) Thermal diffusivity, m2/s Density, kg/m3 Specific heat, kJ/(kg·K)	$kice = 2.2196 - 6.2489 \times 10^{-3}T + 1.0154 \times 10^{-4}T^2$ $\alpha ice = 1.1756 - 6.0833 \times 10^{-3}T + 9.5037 \times 10^{-5}T^2$ $\rho ice = 9.1689 \times 10^2 - 1.3071 \times 10^{-1}T$ $cice = 2.0623 + 6.0769 \times 10^{-3}T$

Table (3) Thermal Property Models for unfrozen composition Data,Initial freezing point [Ashrae 1998]

Food Item	*Moisture Content,%* x_{wo}	*Protein, %* x_p	*Fat, %* x_f	*Carbohydrate, %* x_c	*Fiber, %* x_f	*Ash, %* x_a	*Specific heat above freezing kJ/kg.K*	*Specific heat below freezing kJ/kg.K*	*Initial freezing point, ℃*
Broccoli	*90.7*	*2.98*	*0.35*	*5.24*	*3.00*	*0.92*	*3.85*	*1.97*	*-0.6*
Banana	*74.3*	*1.03*	*0.48*	*23.43*	*2.40*	*0.80*	*3.35*	*1.76*	*-0.8*
Meat	*57.3*	*17.32*	*24.05*	*0.0*	*0.0*	*0.81*	-	-	*-2.2*
Perch	*78.7*	*18.62*	*1.63*	*0.0*	*0.0*	*1.20*	*3.52*	*1.84*	*-2.2*

Table (4) Thermal and Related Properties of Food [Ashrae 1998]

Kind of food	Water content, %(mass)	Highest Freezing point ºC	Latent heat of fusion, kJ/ kg
Broccoli	*90*	*-0.6*	*301*
Banana	*75*	*-0.8*	*251*
Meat	*45*	*-2.2*	*150*
Perch	*80*	*-2.1*	*267*

Table (5) Surface temperature and volume for numerical work [Ashrae 1998]

Kinds of food	T_c surface (^oC)	Cube block Length (m)
Meat, perch, banana and broccoli (purely theoretical)	-10	0.1
	-15	0.1
	-20	0.1
	-15	0.15
	-15	0.2
Meat(experimental Condition)	-9	0.2